Optimization of maghemite-loaded PLGA nanospheres for biomedical applications

Marcela Fernandes Silva †, Ana Adelina Winkler Hechenleitner †,Maite Agüeros ‡, Rebeca Peñalva ‡, Juan Manuel Irache ‡, Edgardo Alfonso Gómez Pineda †*

† Departamento de Química, Universidade Estadual de Maringá, Av. Colombo 5790, 87020-900, Maringá, PR, Brazil; ‡Departamento de Farmacia y Tecnología Farmacéutica, Universidad de Navarra, 31080 Pamplona, Spain, *celafs@gmail.com

ABSTRACT: Magnetic nanoparticles have been proposed as interesting tools for biomedical purposes. One of their promising utilization is the MRI in which magnetic substances like maghemite are used in a nanometric size and encapsulated within locally biodegradable nanoparticles. In this work, maghemite has been obtained by a modified sol-gel method and encapsulated in polymer-based nanospheres. The nanospheres have been prepared by single emulsion evaporation method. The different parameters influencing the size, polydispersity index and zeta potential surface of nanospheres were investigated. The size of nanospheres was found to increase as the concentration of PLGA increases, but lower sizes were obtained for 3 min of sonication time and surfactant concentration of 1%. Zeta potential response of magnetic nanospheres towards pH variation was similar to that of maghemite-free nanospheres confirming the encapsulation of maghemite within PLGA nanospheres. The maghemite entrapment efficiency and maghemite content for nanospheres are 12% and 0.59% w/w respectively.

KEYWORDS: PLGA, maghemite, nanospheres

1. INTRODUCTION

Magnetic nanoparticles (MNPs) have attracted much attention in the last decades for their potential applications in materials science or/and biomedicine. More particularly, due to magnetic properties, this kind of nanoparticles can be used in various special medical techniques such as drug targeting, magnetic resonance imaging (MRI) and magnetic fluid hyperthermia (MFH). [1, 2]

In the last decade, increased investigations with several types of iron oxides have been carried out in the field of MNPs. Thus, the following iron compounds have been proposed to produce MNPs: Fe_3O_4 or magnetite ($Fe^{II}Fe^{III}{}_2O_4$), α-Fe_2O_3 (hematite), γ-Fe_2O_3 (maghemite), FeO (wustite), ε-Fe_2O_3 and β-Fe_2O_3. Among them, MNPs from either magnetite or maghemite are the most promising and popular candidates for biological purposes since their biocompatibility have already been proven. Both types of ferromagnetic nanoparticles may be also superparamagnetic when their size is below 15 nm. [3]

One of the most researched biomedical applications for MNPs is hyperthermia. It has been used as alternative cancer therapy to minimize severe adverse effects of conventional treatments. Hyperthermia of tumors can be achieved using different strategies, such as application of microwave and radio frequency fields or introduction of ferromagnetic needles in the cancer site. Although hyperthermia has been shown to be an extremely powerful anti-cancer agent and a potent radiation sensitizer, the full potential of this therapy is hindered by a number of limitations, as for instance the non-homogeneous distribution of temperature over the cancer site, low specificity, patient discomfort, and thermo-tolerance development. [4] More recently, in order

to overcome the above-mentioned limitations, biocompatible magnetic nanoparticles have been proposed as a material basis to support the development of hyperthermia. [5] For MNPs based hyperthermia, a general procedure involves the distribution of particles throughout the targeted tumor site followed by generation of heat in to the tumor using an applied magnetic field. [6 7] The mechanism of heating can be attributed to the phenomena of relaxation (Néel and Brownian) and hysteresis loss. [8]

In spite of their high hyperthermia efficiency, many MNPs show some drawbacks that may limit their potential use. These inconveniences are related with their large surface-to-volume ratio and, indeed, high surface energies. Consequently, these nanoparticles tend to aggregate in order to minimize their surface energies. Moreover, the naked iron oxide nanoparticles have high chemical activity, and are easily oxidized in air, resulting in loss of magnetism and dispersibility properties. One possible strategy to minimize these drawbacks may be to coat or encapsulate MNPs in polymeric nanospheres and nanocapsules made from biodegradable polymers. These polymers would act as protecting shells, stabilizing the MNPs and, eventually, may be used for further functionalization. In addition, the adequate selection of the coating polymer may permit to prolong the circulation time of the composite and, then, increase the possibilities to MNPs to reach and concentrate in the tumor area. [9]

In this context, synthetic and natural polymers have been extensively researched for the stabilization and functionalization of MNPs. [10] Usually synthetic polymers are preferred because of their purity and reproducibility. Among others, copolymers between lactic and glycolic acids [poly(lactide-co-glycolide) (PLGA)] offer additional advantages such as their biocompatibility and biodegradability to nontoxic metabolites as well as their approval by regulatory agencies (i.e. FDA) for human therapeutic uses. [11]

However, a challenge on the coating of MNPs by polymers is the incompatibility between magnetic particles and PLGA and other biocompatible polymers is that the hydrophobic nature of these compounds hampers the encapsulation of MNPs. In fact, the main problem is how to incorporate, in a high extent, MNPs into PLGA particulates in order to obtain a system capable to be used for hyperthermia purposes. [12] Most studies used iron oxides coated with oleic acid in order to make the surface hydrophobic and thus more compatible with PLGA. [13- 15] Although oleic acid has been recognized as an unsaturated fatty acid with numerous benefits to human health, currently, some articles has been questioning possible risks that this fatty acid may lead to the human body. [16] The findings suggest that exposure of low concentrations of oleic acid negatively affects the barrier function of the intestinal epithelium, including mechanisms that prevent absorption of potentially toxic substances common in food. [17- 19]

Because of this, the challenge of this study was to develop a procedure to entrap iron oxide magnetic nanoparticles in PLGA nanospheres in the absence of toxic or irritant compounds (i.e. oleic acid). In addition we have focused our study on the optimization of nanospheres and nanocapsules production. In particular, the effects of sonication time, surfactant, polymer and iron oxide amount have been investigated with respect to their impact on the physico-chemical characteristics of the resulting MNPs-loaded PLGA nanospheres.

2. EXPERIMENTAL

2.1 Materials

Ferric nitrate ($Fe(NO_3)_3.9H_2O$) (Vetec, Brazil), poly(vinyl alcohol) (PVA; MW 146,000-180,000 88-89% hydrolyzed) (Aldrich,USA) , Pluronic F-68 (Sigma-Aldrich, USA), Poly-lactic-co-glycolic acid with a monomer ratio of 50:50 (Resomer® RG 502, Boehringer Ingelheim,

Germany), ethyl acetate (99%- Panreac, Spain), dichlorometane (99%, Merck, Germany) sodium citrate tribasic dehydrate (ACS 99%- Sigma Aldrich, USA), sucrose (Fragon, Spain).

2.2 Synthesis of maghemite nanoparticles (Mag)

The maghemite nanoparticles (Mag) were synthetized by a modified sol-gel method.[20] Aqueous diluted PVA (10% w/v) and saturated ferric nitrate solutions were separately prepared and then mixed at specific metallic ion/monomer unit ratios. The solutions were maintained at room temperature under stirring for 2 h and then heated under vigorous stirring until total water evaporation. The temperature was maintained at 150°C for thermal degradation of the polymer. The nanostructured material was obtained after calcination of the material under air atmosphere at 400°C for 4h.

2.3 Preparation of maghemite loaded-PLGA nanospheres (MagPLGA-NE)

PLGA nanospheres loaded with Mag were prepared by a single emulsion method previously described.[21] For this purpose, Mag was dispersed by sonication (Microson ultrasonic cell disruptor XL, Misonix, USA) in 0.5 ml of ethyl acetate for 1 min. This suspension was then mixed with a solution of PLGA in the same solvent. The organic phase was then emulsified by sonication in 3 mL of an aqueous solution of PVA. The resulting suspensions were stirred with a blade stirrer at room temperature in order to eliminate the organic solvent. The resulting nanoparticles were, firstly, centrifuged at 1,000 rpm for 20 min in order to eliminate unloaded Mag and, secondly, were washed two times with distilled water by consecutive centrifugation (Biofuge Stratus, Heraeus Instruments, Germany) at 17,000 r.p.m. for 10 min at 4ºC. The pellet was then dispersed in 3 ml aqueous solution containing 5% sucrose as cryoprotector. The formulations were freeze-dried in a Genesis 12EL apparatus (Virtis, USA). Empty PLGA

nanospheres (PLGA-NE) were prepared as described above without using Mag and used as control.

2.4 Physico-chemical characterization

X-ray measurements were carried out on a Siemens-5000 powder diffractometer with monochromated Cu $K_{\alpha 1}$ radiation (λ=1.54056Å). Reflection x-ray powder diffraction data were collected from 10° to 90° in 2h. The size of maghemite nanoparticles was calculated based on the full-width at half maximum of (220) preferred orientation using the Scherrer equation (equation 1): [22]

$$d = \frac{K\lambda}{(B cos\theta_B)} \qquad (1)$$

where λ is the X-ray wavelength, κ the shape factor, D the average diameter of the crystals, θ_B the Bragg angle, and B is the line broadening measured at half-height.

The value of κ depends on several factors, including the Miller index of the reflecting plane and the shape of the crystal. If the shape is unknown, κ is often assigned a value of 0.89

FTIR spectra were obtained using a FTIR BOMEM MB 100 spectrometer (Quebec, Canada) with samples in 1% KBr pellets, operating from 4000 to 400 cm^{-1}, at resolution of 4 cm^{-1}.

The size and zeta potential of Mag nanoparticles and Mag-loaded PLGA nanospheres were determined by photon correlation spectroscopy and electrophoretic laser Doppler anemometry, respectively, using a Zetamaster analyzer system (Malvern Instruments, UK). For size measurements, samples were dispersed with deionized water and measured at 25 °C with a scattering angle of 90° and for zeta potential measurements, samples were dispersed in aqueous solution of KCl 0.3mM at pH 3-10. The mean hydrodynamic diameter was obtained by fitting the autocorrelation function with the cumulant method, which also gives the polydispersity index (PDI) (equation 2), which is defined as: [23]

$$PDI = \frac{R_{i-1}R_{i+1}}{(R_i)^2} \qquad (2)$$

where Ri is the ith moment of the particle size distribution.

For average diameter measurements the error bar indicates the width of the distribution and for the PDI measurements the error bar indicates the standard deviation calculated from three measurements.

The shape and morphology of nanoparticles and nanospheres were assessed by electron microscopy. Mag nanoparticles were observed by TEM in a JEM-1400 apparatus (JEOL, Tokyo, Japan). For this purpose, samples were diluted with methanol and placed on a formvar/Carbon 400 mesh, copper grid (Tedpella) without any staining. Then the drops were dried at room temperature and visualized in the apparatus. For Mag-loaded PLGA nanospheres, they were negatively stained with phosphotungstic acid before observation in the TEM apparatus (EM10, Zeiss, USA) after negative staining of the samples with phosphotungstic acid. On the other hand, particles were also examined by using a Field Emission Scanning Electron Microscope (Carl Zeiss Ultra Plus, Germany). In this case, samples were mounted on Carbon coated TEM copper grids (carbon films on 3mm 400 mesh grids, Agar Scientific) and placed in a desiccator in order to evaporate water. Finally, the grids were adhered with a double-sided adhesive tape onto metal stubs for SEM visualization.

2.5 Amount of Mag-loaded in nanospheres

To determine the amount of maghemite nanoparticles encapsulated in the PLGA composites, 20 mg of Mag-loaded PLGA nanospheres were digested in 20 mL HCl 18.5% during 2 h at 70ºC. The resulting mixtures were diluted in distilled water and the iron concentration in samples was quantified by atomic absorption spectrophotometry (AAS) at 248.4 nm using acetylene-air flame

in a Varian AA10 plus apparatus (Varian, Australia). The assay was linear between 0 and 8 μg/ml with a correlation coefficient of 1.0

Loaded maghemite in optimized MagPLGA nanospheres were calculated from the amount of iron measured by AAS. Maghemite entrapment efficiency (%) and maghemite content (% w/w) were calculated by equations 3 and 4, respectively:

Maghemite entrapment efficiency (%):

$$= \frac{Mass\ of\ maghemite\ in\ MagPLGA\ nanospheres}{Mass\ of\ maghemite\ used\ in\ formulation} \quad (3)$$

Maghemite content (% w/w):

$$= \frac{Mass of maghemite in MagPLGA nanospheres}{Mass of MagPLGA nanospheres} \quad (4)$$

3. RESULTS AND DISCUSSION

3.1 Characterization of maghemite nanoparticles

The chemical structure of maghemite was studied by X-ray diffraction and FTIR. Figure 1 shows a XRD spectrum of Mag nanoparticles. The diffraction pattern obtained for the synthesized maghemite was similar to that described for the standard γ-Fe_2O_3 crystal (JCPDS 39-1346). The well-defined X-ray diffraction pattern indicates the formation of highly crystallized iron oxide. γ-Fe_2O_3 particles have cubic unit cells with both octahedrally and tetrahedrally coordinated Fe^{3+} sites (defect spinel structure), and the diffraction planes were attributed in Figure 1. The synthesized nanoparticles displayed an average size of 15 nm.

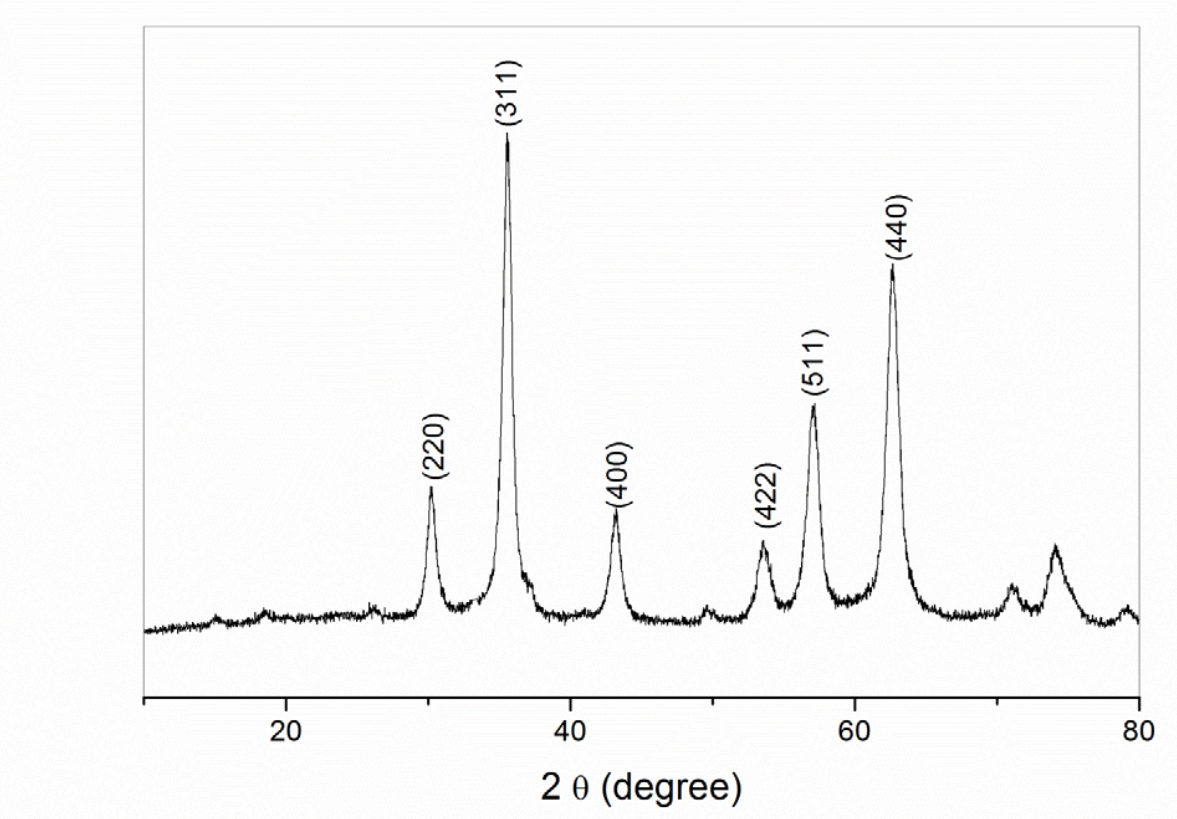

Figure 1: XRD patterns of obtained maghemite.

Figure 2 shows the FTIR spectrum of Mag nanoparticles. The broadly band at 3000-3700 cm^{-1} is characteristic of hydroxyl (-OH) surface groups of γ-Fe_2O_3, whereas the peaks at 1400-1600 cm^{-1} are due to residual nitrate ions. The bands between 400-600 cm^{-1} are assigned Fe-O stretching and bending vibration mode, respectively of γ-Fe_2O_3. [24]

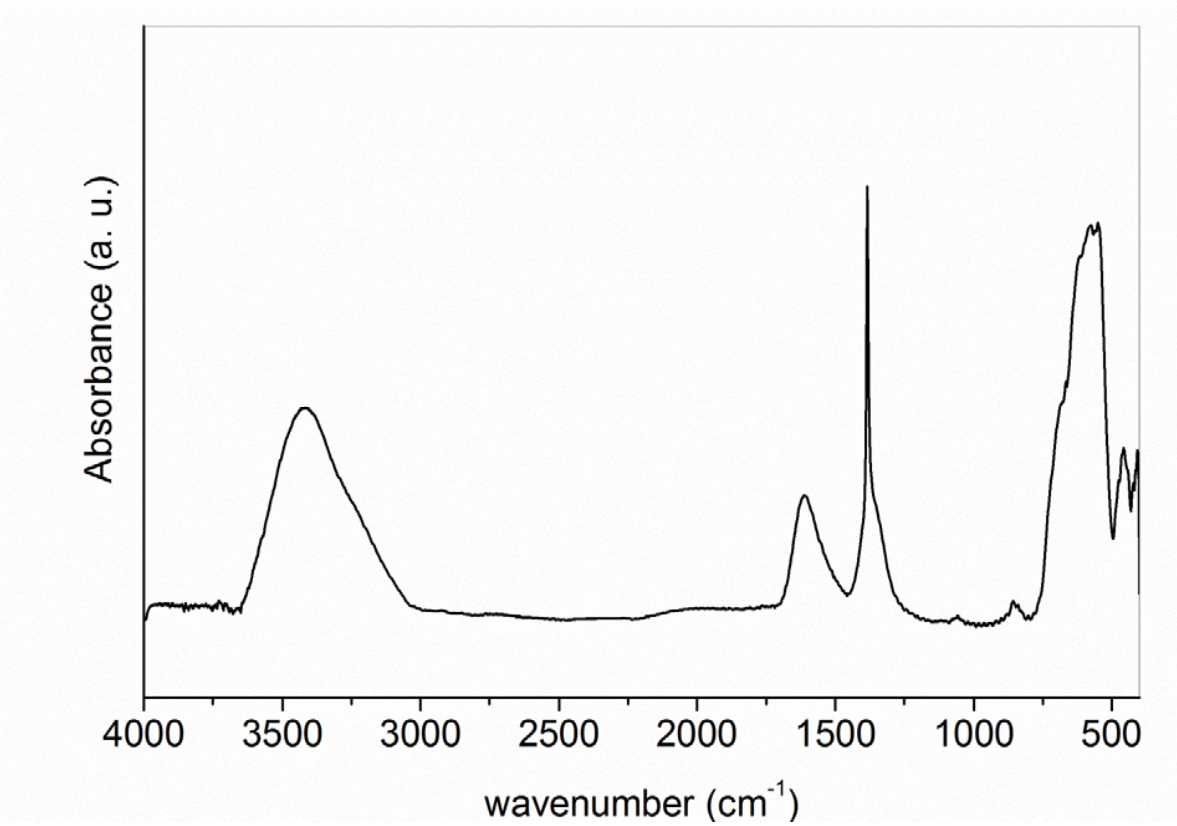

Figure 2: FTIR spectrum of obtained maghemite

The morphology of Mag nanoparticles was also analyzed by TEM (Figure 3). Mag nanoparticles presented a cubic shape with a mean size of about 15 nm, in agreement with the XRD calculated size.

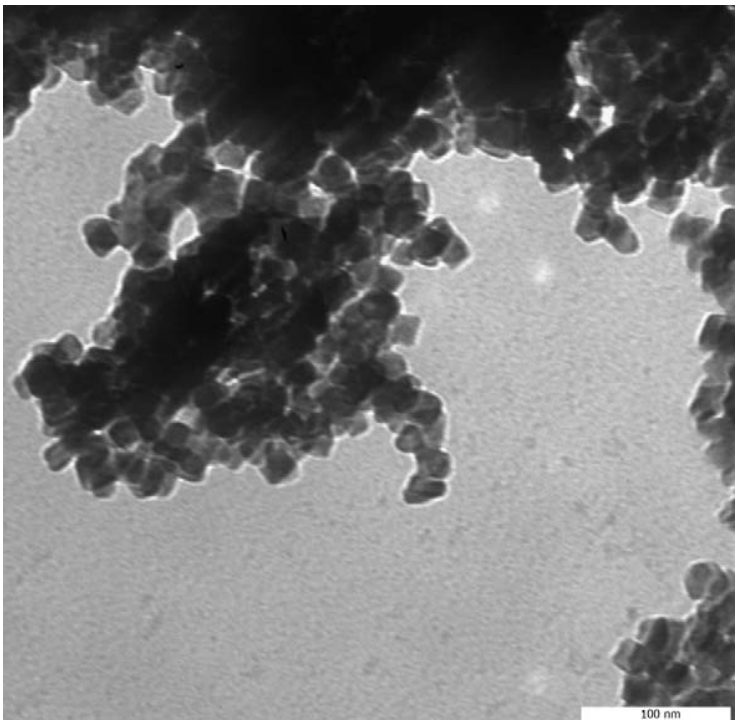

Figure 3: TEM image from maghemite nanoparticles.

3.2 Optimization of Maghemite-loaded PLGA nanospheres

In order to optimize the preparative process of Mag-loaded PLGA nanospheres and, thus, to obtain homogeneous particulates with a maximum of maghemite content, various formulation parameters were investigated. Thus, the effect of the PLGA amount, PVA concentration, initial amount of MNPs and time of sonication for the emulsification process on the physico-chemical characteristics of the resulting nanospheres were evaluated. The effect of some of these parameters, such as surfactant concentration, oil-to-water phase ratio, polymer molecular weight, polymer concentration and stirring rate have already been studied. [25, 26] However, most of these studies have just been applied for the encapsulation of a drug into polymeric nanoparticles rather than other nanoparticles in nanospheres.

The sonication time at a frequency of 20 kHz were varied in 1, 3 and 5 min. [PLGA] was varied in 100, 200 and 400 mg/mL. [PVA] in aqueous phase was varied in 0.5, 1 and 2% and the initial ratio of maghemite/PLGA was varied in 0.02, 0.05 and 0.1mg/mg.

3.2.1 Sonication time during the emulsification step

The sonication time is of great importance, because if sonication is not applied for sufficiently long time, the resulting particle size distribution will be broad. The ultrasonication is characterized by a complex dynamics of collisions, coalescence, and breakage of droplets, which reaches a dynamic equilibrium only after a sufficient time that increases as the emulsifier concentration decreases. Afterwards, the droplet size distribution stabilizes, being usually characterized by a low polydispersity in the final emulsion. [27]

Figure 4 shows the influence of the sonication on the emulsification process of the organic phase (containing PLGA and Mag) into the aqueous phase of PVA. As it can be shown, the time of sonication influenced the average size, PDI and zeta potential of the resulting nanospheres. According to these data, the optimum time of sonication for the preparation of these nanospheres was 3 minutes. Under these experimental conditions, the mean size of the resulting nanospheres was close to 200 nm and the PDI was around 0.1. Although the literature reports that longer sonication times induce the formation of smaller particles, we must consider that the energy generated by sonication process may result in an increase of temperature in the area closer to the ultrasonic tip, leading to changes in the physical properties of the polymer, resulting in the formation of aggregates (like as observed for 5 min of sonication). [28- 29] Despite of the ice bath used in the sonication process , the obtained cooling may not be sufficient to maintain a stable temperature in the area near the source of energy (ultrasound tip), due to the rate of the temperature gradient in the polymer, resulting the formation of aggregates. Concerning the zeta

potential, the time of sonication displayed a low influence in this parameter and small differences between the different nanospheres produced were found. In addition, the resulting values of zeta potential for the Mag-loaded PLGA nanospheres (in a range between -4.5 and -8 mV) are in agreement with previous data reported by other authors. [30- 31] PDI (which indicates the size distribution of the nanospheres), with values lower than 0.3 normally are considered satisfactory.[32]

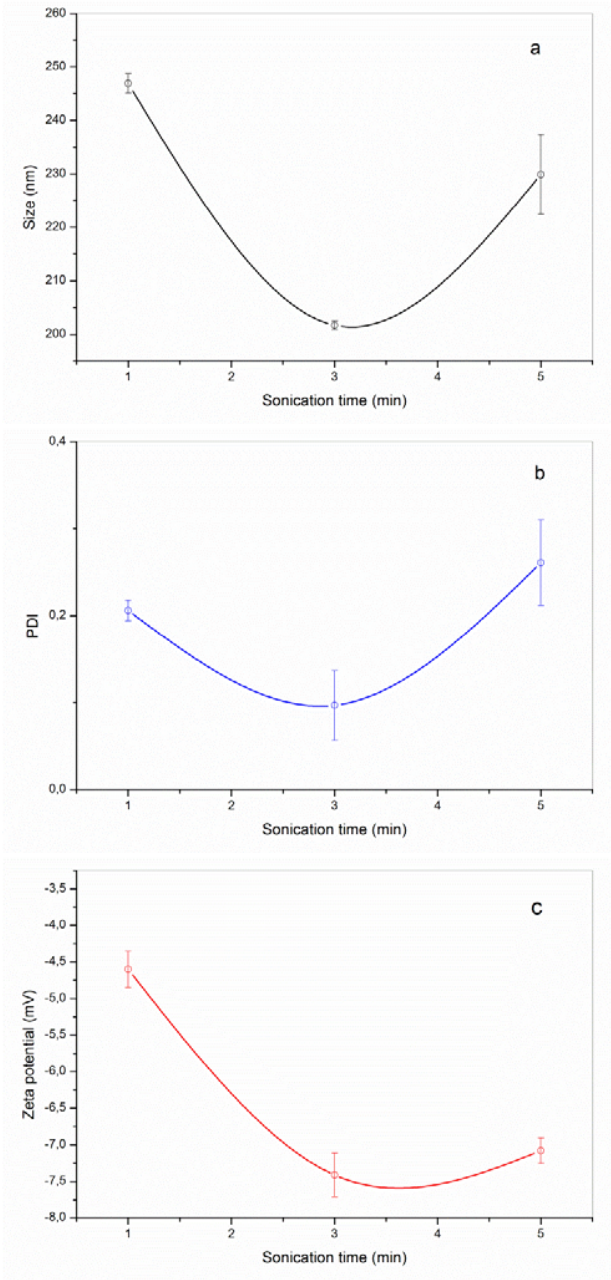

Figure 4: Influence of the time of emulsification by sonication on a) the mean hydrodynamic size, b) polydispersity index and c) zeta potential (measured at pH 7) of the resulting Mag-loaded PLGA nanospheres. Data expressed as mean ± SD (n = 3). Experimental conditions: PLGA: 100 mg; initial Mag added: 5 mg; PVA concentration:1% w/v.

3.2.2 PVA concentration in the aqueous phase

The amount of emulsifier is probably the parameter that most strongly determines the theoretical final particle size. It is well known that an increasing amount of emulsifier leads to a decrease of particle size, until a minimum value is reached. [33] While this behavior is general, the type of emulsifier is playing an important role, since it is also known that ionic emulsifiers are more effective in stabilizing small particles as compared to non-ionic emulsifiers.[25] However, most of the FDA approved emulsifiers are non-ionic, and we have focused on PVA because it is one of the most commonly used emulsifiers in the pharmaceutical industry. In order to demonstrate the effect of the emulsifier on the particle size and size distribution in our system, its concentration was varied in 0.5, 1 and 2%. Results are shown in Figure 5.

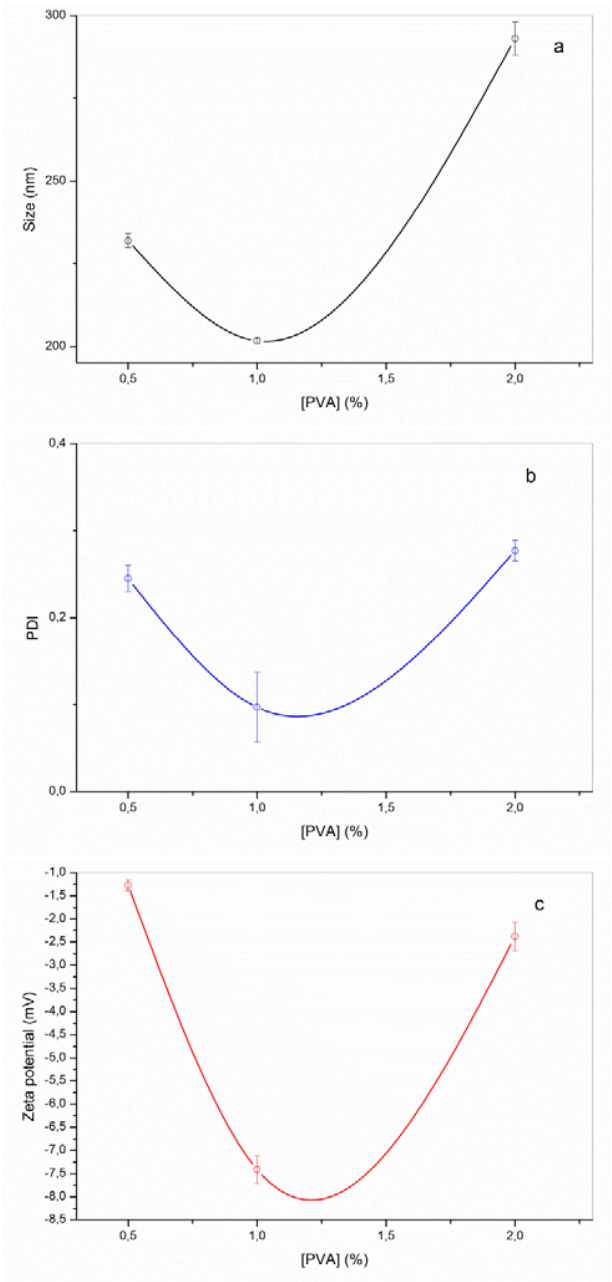

Figure 5: Influence of the PVA concentration on a) the mean hydrodynamic size, b) polydispersity index and c) zeta potential (measured at pH 7) of the resulting Mag-loaded PLGA nanospheres. Data expressed as mean ± SD (n = 3). Experimental conditions: PLGA: 100 mg; initial Mag added: 5 mg; Time of sonication: 3 min.

When the concentration of PVA in the aqueous phase was 1% w/v, the resulting nanospheres displayed the smaller mean size but with the highest homogeneicity. However, with the increase in PVA concentration, the viscosity of the external aqueous phase increased in the same way, which resulted in size increase due to decrease in the net shear stress. [34, 35] At a high PVA concentration (2%), more molecules of PVA may be oriented in organic solvent/water interface to reduce efficiently the interfacial tension which resulted in significant increase in the net shear stress at a constant energy density during emulsification and promoted the formation of smaller emulsion droplets

PDI values lower than 0.3 are satisfactory and zeta potential variation in the range of -3 and -8 mV is in agreement with the behavior of the material.

3.2.3 PLGA concentration

PLGA concentration in organic phase was varied between 50 and 200 mg/mL, and the influence of [PLGA] on the particles size and size distribution was studied. The results are shown in Figure 6. As expected, the size of PLGA nanospheres increased by increasing the amount of the polymer. This observation is in agreement with previously published reports. [36- 38] This fact has been related with the increasing viscosity of the dispersed phase (polymer solution), resulting in a poorer dispersability of the PLGA solution into the aqueous phase. [37] As a consequence, this increased viscosity would induce a high resistance against the shear forces during the emulsification process, yielding coarse emulsions, which lead to the generation of bigger droplets.

In addition, by increasing the amount of PLGA, PVA was probably insufficient to cover the surface of droplets completely, which caused the coalescence of droplets during the evaporation of organic solvent and aggregation of nanoparticles after the removal of organic solvent.[33]

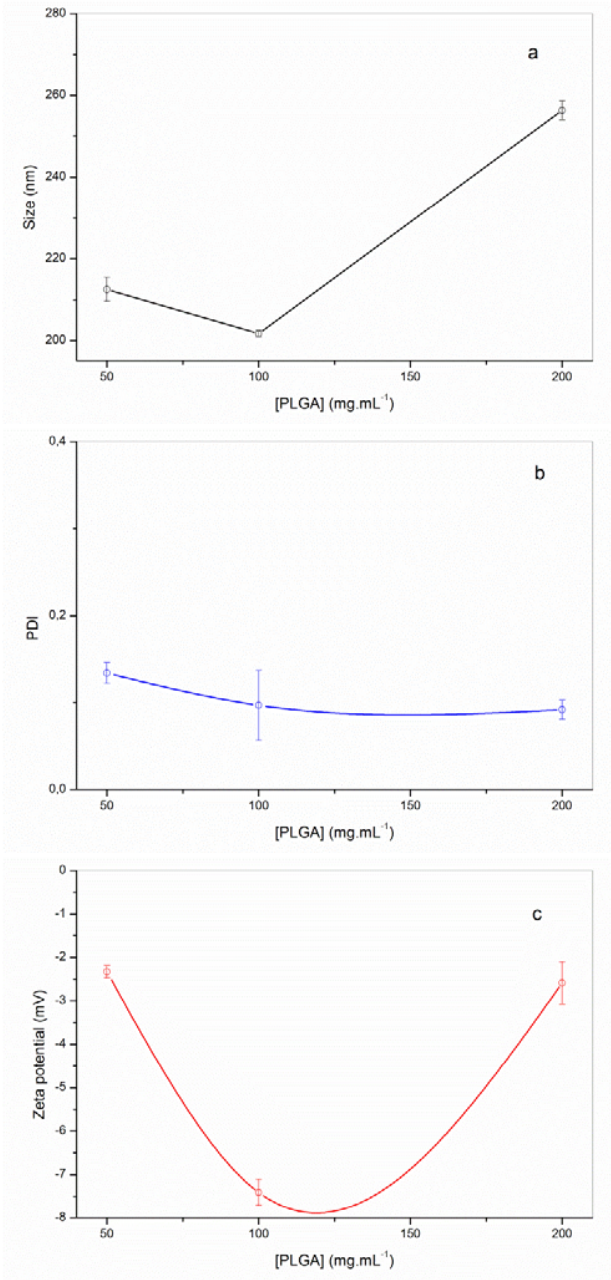

Figure 6: Influence of the PLGA concentration on a) the mean hydrodynamic size, b) polydispersity index and c) zeta potential (measured at pH 7) of the resulting Mag-loaded PLGA nanospheres. Data expressed as mean ± SD (n = 3). Experimental conditions: initial Mag added: 5 mg; PVA concentration: 1% w/v, Time of sonication: 3 min.

3.2.4 Maghemite amount

The initial maghemite/PLGA ratio was varied in the range 0 to 0.10 mg/mg and the influence of this parameter on the size, polydispersibility and zeta potential was evaluated. Surprinsingly, the amount of Mag used to prepare PLGA nanospheres did not influenced significantly the physico-chemical properties of the resulting particulates. In all case, the resulting mean sizes were around 240 nm with a polydispersity lower than 0.2 and zeta potential data of about -2 to -8 mV.

After this optimization study, the following experimental conditions for the preparation of PLGA nanospheres were selected: PLGA amount (100 mg), Mag amount (5 mg), PVA concentration (1% w/v) and a time of sonication for the emulsification process of 3 minutes. Under these experimental conditions the resulting Mag-loaded PLGA nanospheres displayed a mean size of 200 nm, a maghemite content of 59 µg per mg nanosphere and an encapsulation efficiency of 12% (Table 1). Figures 7 and 8 shows the morphological characterization of these nanospheres by SEM and TEM respectively.

Table 1. Physico-chemical characteristics of PLGA nanospheres. Data expressed as mean ± SD (n = 3). Experimental conditions: PLGA amount: 100 mg, initial Mag added: 5 mg; PVA concentration: 1% w/v, Time of sonication: 3 min.

Sample	Hydrodinamic size (nm)	PDI	Zeta Potential (mV)	Mag loading ($\mu g.mg^{-1}$)	Encapsulation efficiency(%)
PLGA-NE	210 ± 2.1	0.185 ± 0.03	-6.27 ± 0.3	-	-
MagPLGA-NE	202 ± 0.81	0.097 ± 0.04	-7.41 ± 0.3	59	12

Mag-loaded PLGA nanospheres were found to be spherical with an average size of about 200 nm; similar to the size determined by photon correlation spectroscopy. The maghemite

nanoparticles encapsulated in nanospheres appeared to be well dispersed inside the PLGA nanospheres.

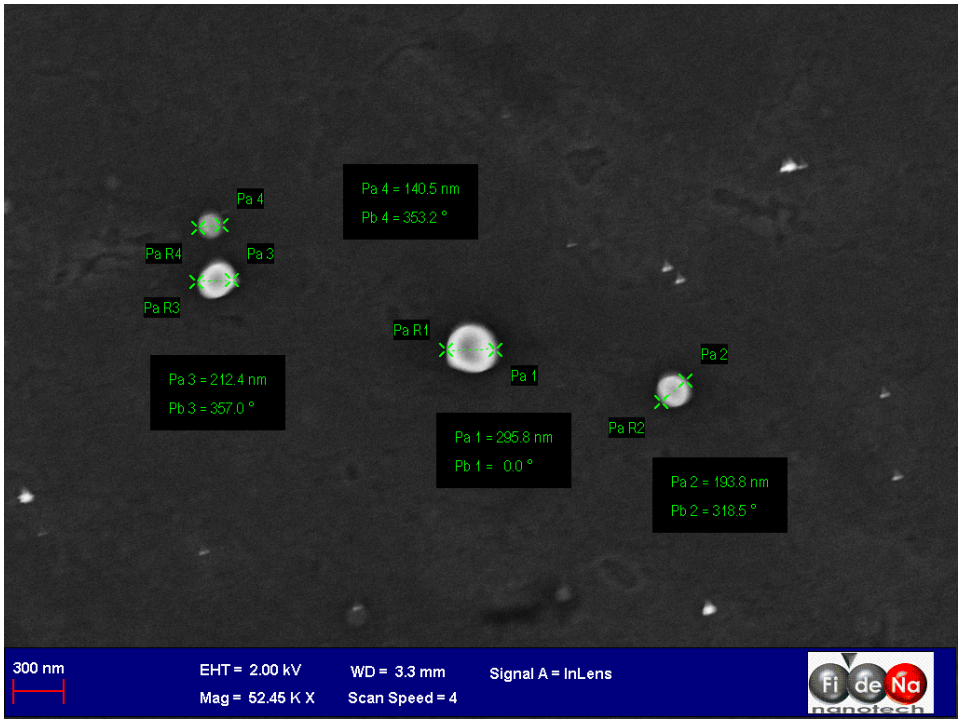

Figure 7: SEM micrograph of Mag-loaded PLGA nanospheres

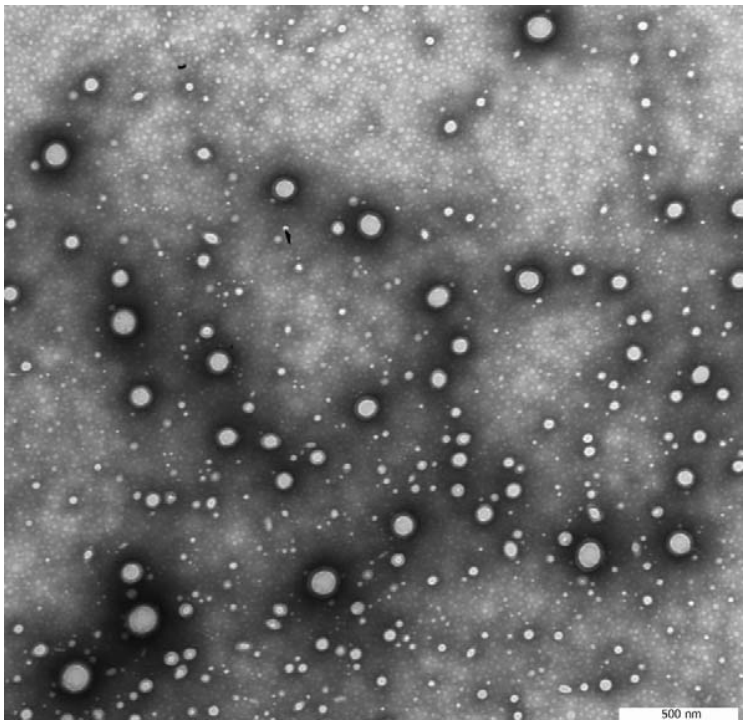

Figure 8: TEM micrograph of Mag-loaded PLGA nanospheres

In order to investigate the efficiency of the entrapment of magnetic nanoparticles in the polymeric nanospheres, we have compared the surface properties of empty PLGA nanospheres with Mag-loaded PLGA nanospheres and pure maghemite. Previously, Arias and collaborators have proposed the electrophoresis measurement of poly(ethyl-2-cyanoacrylate) nanoparticles with a magnetic core as a useful tool for qualitatively checking the efficiency of the magnetite coating by the polymer. [39] For this purpose, the zeta potential of empty PLGA nanospheres, MagPLGA nanospheres and pure maghemite was assessed as a function of pH in the presence of 0.3 mM KCl. Figure 9 summarized these results. When the pH of the medium increases from 3 to 9, the zeta potential of Mag-loaded and empty PLGA nanospheres slightly decreased due to the dissociation of negative charge generating groups like carboxylic groups of PLGA polymer. [13] Then, from pH 9 to 11, the zeta potential of the Mag-PLGA nanospheres was in the same order

of magnitude to that of empty PLGA nanospheres. On the contrary, the zeta potential values for pure maghemite decreased sharply by increasing the pH conditions. Considering an iron oxide surface in contact with water, a fully hydroxylated surface should be expected. The net charge of the iron oxide surface is dependent on the protonation/deprotonation of the hydroxyl groups when the pH of the solution changes. [40] In any case, these results confirmed that maghemite was totally encapsulated in the resulting PLGA nanospheres. These findings are in agreement with previous determinations described by Okassa and collaborators working with magnetite/maghemite PLGA composite particles. [13]

As observed, for Mag, Mag loaded PLGA nanospheres and empty PLGA nanospheres, the data suggest an isoeletric point below pH 2. This small value of isoelectric point for maghemite can be due the presence of hydroxyl groups on nanoparticles surface, in agreement with the results showed by FTIR spectra, in Figure .

PLGA nanospheres always bear a net negative surface charge, and our data suggest an isoelectric point below pH 2. The electrokinetic properties of Mag loaded PLGA nanospheres is in good coincidence with those of pure PLGA, as one would predict in case of an optimum coverage. [41]

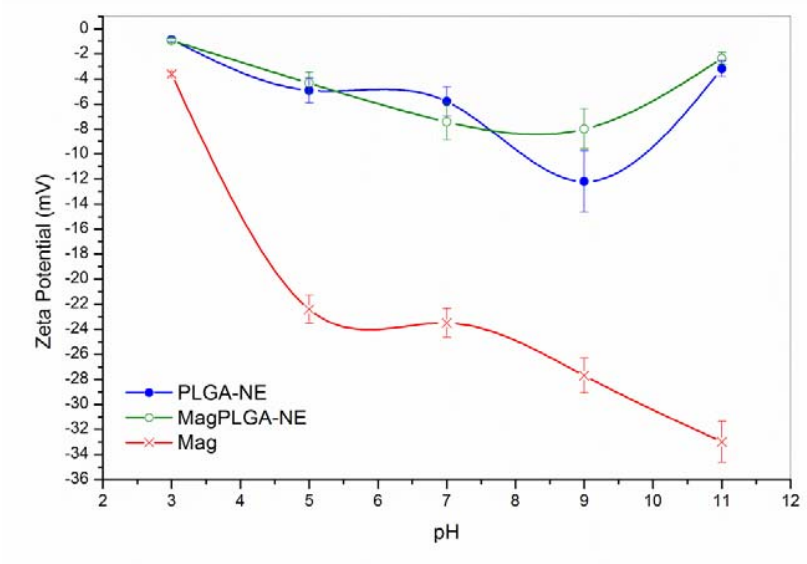

Figure 9: Evolution of the zeta potential of particulates as a function of the pH medium.

4. CONCLUSIONS

The emulsion-solvent evaporation method allowed the preparation of spherical maghemite-loaded systems of biodegradable PLGA. The influences of various processing variables on particle size, polydispersity and surface zeta potential were systematically assessed. It was concluded that formulation variables could be exploited in order to enhance the properties previously cited for PLGA nanospheres. Based on the optimal parameters, it was found that MagPLGA with expectable properties (average sizes of 200 and 240 nm respectively for MagPLGA-NE and MagPLGA-NC and polydispersity lower than 0.3 for both) could be obtained. We point out that maghemite (a hydrophilic molecule) could be entrapped into PLGA nanospheres and maghemite content (% w/w) respectively of 0.59 and 0.44, consistent with those previously reported in the literature.

5. AUTHOR INFORMATION

Corresponding Author

*celafs@gmail.com

Present Addresses

† Departamento de Química, Universidade Estadual de Maringá, Av. Colombo 5790, 87020-900, Maringá, PR, Brazil; ‡Departamento de Farmacia y Tecnología Farmacéutica, Universidad de Navarra, 31080 Pamplona, Spain,

Author Contributions

The manuscript was written through contributions of all authors. All authors have given approval to the final version of the manuscript.

6. ACKNOWLEDGMENT

The authors thank the financial support of Capes - DGU 184-09 and MCI Spain – PHB 2008-0044-PC.

7. ABBREVIATIONS

MNPs magnetic nanoparticles, MRI magnetic resonance imaging, MFH magnetic fluid hyperthermia, PLGA Poly-lactic-co-glycolic acid, FDA Food and Drugs Administration, PVA Poly(vinyl alcohol), PDI Polydispersity index, TEM transmission electronic microscopy, SEM Scanning Electronic microscopy, Mag maghemite, PLGA-NE PLGA nanospheres MagPLGA-NE Mag loaded PLGA nanospheres, XRD X-ray Diffraction, AAS Atomic Absorption Spectrophotometry, FTIR Fourier Transform Infrared Spectroscopy.

8. SYNOPSIS

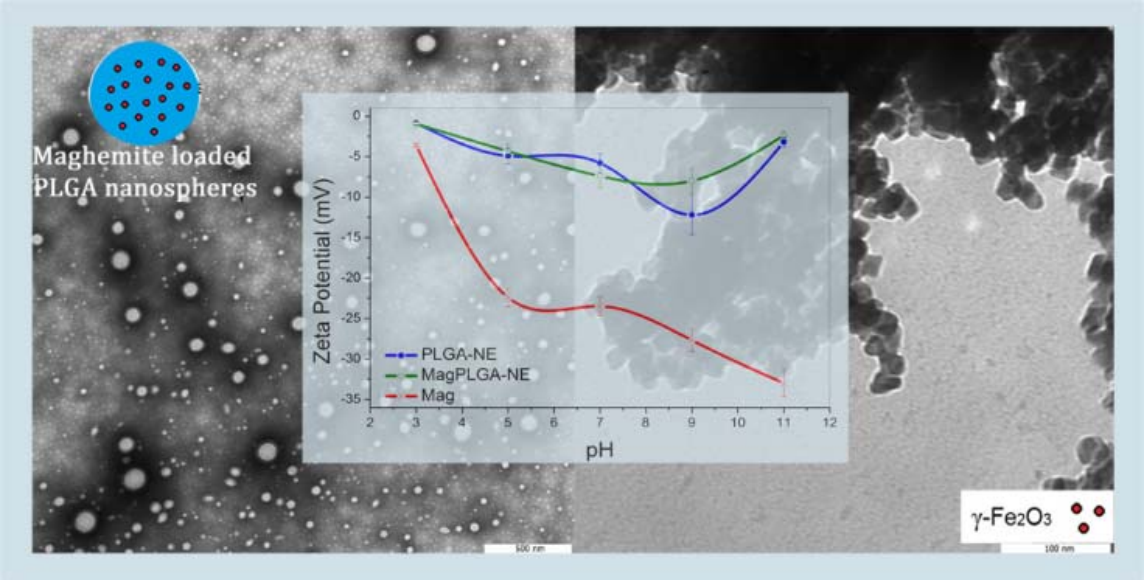

9. REFERENCES

1. Salazar, J. S.; Perez, L.; Abril, O. d.; Phuoc, L. T.; Ihiawakrim, D.; Vazquez, M.; Greneche, J.-M.; Begin-Colin, S.; Pourroy, G. Magnetic Iron Oxide Nanoparticles in 10−40 nm Range: Composition in Terms of Magnetite/Maghemite Ratio and Effect on the Magnetic Properties. Chem. Mater. 2011, 23, 1379–1386.

2. Hu, M.; Belik, A. A.; Imura, M.; Mibu, K.; Tsujimoto, Y.; Yamauchi, Y. Synthesis of Superparamagnetic Nanoporous Iron Oxide Particles with Hollow Interiors by Using Prussian Blue Coordination Polymers. Chem. Mater. 2012, 24, 2698–2707.

3. Wu, W.; He, Q.; Jiang, C. Magnetic Iron Oxide Nanoparticles: Synthesis and Surface Functionalization Strategies. Nanoscale Res. Lett. 2008, 3, 397-415.

4. Calderwood, S. K.; Asea, A. Targeting HSP70-induced thermotolerance for design of thermal sensitizers. Int. J. Hyperthermia 2002, 18, 597-608.

5. Guedes, M. H. A.; Guedes, M. E. A.; Morais, P. C.; Silva, M. F. D.; Santos, T. S.; Jr, J. P. A.; Bertelli, C. E.; Azevedo, R. B.; Lacava, Z. G. M. Proposal of a magnetohyperthermia system: preliminary biological tests. J. Magn. Magn. Mater, 2004, 272-276, 2406–2407.

6. Levy, M.; Quarta, A.; Espinosa, A.; Figuerola, A.; Wilhelm, C.; García-Hernández, M.; Genovese, A.; Falqui, A.; Alloyeau, D.; Buonsanti, R.; Cozzoli, P. D.; García, M. A.; Gazeau, F.; Pellegrino, T. Correlating Magneto-Structural Properties to Hyperthermia Performance of Highly Monodisperse Iron Oxide Nanoparticles Prepared by a Seeded-Growth Route. Chem. Mater. 2011,23, 4170–4180.

7. Pankhurst, Q. A.; Connolly, J.; Jones, S. K.; Dobson, J. Applications of magnetic nanoparticles in biomedicine. J. Phys. D- Appl. Phys. 2003, 36, R167.

8. Botez, C. E.; Morris, J. L.; Eastman, M. P. Superspin relaxation in Fe3O4/hexane magnetic fluids: A dynamic susceptibility study. Chem. Physics 2012, 89–93.

9. Jia, Y.; Yuan, M.; Yuan, H.; Huang, X.; Sui, X.; Cui, X.; Tang, F.; Peng, J.; Chen, J.; Lu, S.; Xu, W.; Zhang, L.; Guo, Q. Co-encapsulation of magnetic Fe3O4 nanoparticles and doxorubicin into biodegradable PLGA nanocarriers for intratumoral drug delivery. Int. J. Nanomed. 2012, 7, 1697–1708.

10. Kumar, C. S. S. R.; Mohammad, F. Magnetic nanomaterials for hyperthermia-based therapy and controlled drug delivery. Adv. Drug Deliver. Rev. 2011, 63, 789–808.

11. Mundargi, R. C.; Babu, V. R.; Rangaswamy, V.; Patel, P.; Aminabhavi, T. M. Nano/micro technologies for delivering macromolecular therapeutics using poly(d,l-lactide-co-glycolide)

and its derivatives. J. Control. Release 2008, 125, 193–209.

12. Okassa, L. N.; Marchais, H.; Douziech-Eyrolles, L.; Cohen-Jonathan, S.; Soucé, M.; Dubois, P.; Chourpa, I. Development and characterization of sub-micron poly(d,l-lactide-co-glycolide) particles loaded with magnetite/maghemite nanoparticles. Int. J. Pharm. 2005, 302, 187-196.

13. Okassa, L. N.; Marchais, H.; Douziech-Eyrolles, L.; Hervé, K.; Cohen-Jonathan, S.; Munnier, E.; Soucé, M.; Linassier, C.; Dubois, P.; Chourpa, I. Optimization of iron oxide nanoparticles encapsulation within poly(d,l-lactide-co-glycolide) sub-micron particles. Eur. J. Pharm. BioPharm. 2007, 67, 31–38.

14. Astete, C. E.; Kumar, C. S. S. R.; Sabliov, C. M. Size control of poly(d,l-lactide-co-glycolide) and poly(d,l-lactide-co-glycolide)-magnetite nanoparticles synthesized by emulsion evaporation technique. Colloid. Surface A: 2007,299, 209–216.

15. Liu, X.; Kaminski, M. D.; Chen, H.; Torno, M.; Taylor, L.; Rosengart, A. J. Synthesis and characterization of highly-magnetic biodegradable poly(d,l-lactide-co-glycolide) nanospheres. J. Control. Release 2007, 119, 52-58.

16. Ilbäck, N. G.; Nyblom, M.; Carlfors, J.; Fagerlund-Aspenström, B.; Tavelin, S.; Glynn, A. W. Do surface-active lipids in food increase the intestinal permeability to toxic substances and allergenic agents? Med. Hypotheses 2004, 63, 724-730.

17. Aspenström-Fagerlund, B.; Tallkvist, J.; Ilbäck, N.-G.; Glynn, A. W. Oleic acid decreases BCRP mediated efflux of mitoxantrone in Caco-2 cell monolayers. Food Chem. Toxicol.

2012, 50, 3635-3645..

18. Aspenstrom-Fagerlund, B.; Ring, L.; Aspenstrom, P.; Tallkvist, J.; Ilback, N.-G.; Glynn, A. W. Oleic acid and docosahexaenoic acid cause an increase in the paracellular absorption of hydrophilic compounds in an experimental model of human absorptive enterocytes. Toxicol. 2007, 237 12-23.

19. Aspenström-Fagerlund, B.; Sundström, B.; Tallkvist, J.; Ilbäck, N.-G.; Glynn, A. W. Fatty acids increase paracellular absorption of aluminium across Caco-2 cell monolayers. Chem-Biol. Interact. 2009, 181, 272-278.

20. Fernandes, D. M.; Winkler Hechenleitner, A. A.; Silva, M. F.; Lima, M. K.; Stival Bittencourt, P. R. Preparation and characterization of NiO, Fe2O3, Ni0.04Zn0.96O and Fe0.03Zn0.97O. Mater. Chem. Phys., 2009, 118, 447–452.

21. Yang, J.; Park, S. B.; Yoon, H.; Huh, Y. M.; Haam, S. Preparation of poly ε-caprolactone nanoparticles containing magnetite for magnetic drug carrier. Int. J. Pharm. 2006, 324, 185-190.

22. Weibel, A.; Bouchet, R.; Boulc'h, F.; Knauth, P. The Big Problem of Small Particles: A Comparison of Methods for Determination of Particle Size in Nanocrystalline Anatase Powders. Chem. Mater. 2005, 17, 2378–2385.

23. Furlan, M.; Kluge, J.; Mazzotti, M.; Lattuada, M. Preparation of biocompatible magnetite–PLGA composite nanoparticles using supercritical fluid extraction of emulsions. J. Supercrit. Fluid. 2010, 54, 348–356.

24. Sahoo, S. K.; Agarwal, K.; Singh, A. K.; Polke, B. G.; Raha, K. C. Characterization of γ- and α-Fe2O3 nano powders synthesized by emulsion precipitation-calcination route and rheological behaviour of α-Fe2O3. Int. J. Eng. Sci. Technol. 2010, 2, 118-126.

25. Musyanovych, A.; Schmitz-Wienke, J.; Mailander, V.; Walther, P.; Landfester, K. Preparation of biodegradable polymer nanoparticles by miniemulsion technique and their cell interactions(2008), pp. 127–139. Macromol. Biosci. 2008, 8, 127–139.

26. Kluge, J.; Fusaro, F.; Casas, N.; Muhrer, G.; Mazzotti, M. Production of PLGA micro- and nanocomposites by supercritical fluid extraction ofemulsions. I. Encapsulation of lysozyme. J. Supercrit. Fluid. 2009, 50, 327–335.

27. Antonietti, M.; Landfester, K. Polyreactions in miniemulsions. Prog. Polym. Sci., 2002, 27, 689–757.

28. Tripathi, A.; Gupta, R.; Saraf, S. A. PLGA Nanoparticles of Anti Tubercular Drug: Drug Loading and Release Studies of a Water in soluble drug. Int. J. PharmTech Res. 2010, 2, 2116-2123.

29. MUKERJEE, A.; VISHWANATHA, J. K. Formulation, Characterization and Evaluation of Curcumin-loaded PLGA Nanospheres for Cancer Therapy. Anticancer Res. 2009, 29, 3867-3876.

30. Cohen-Sela, E.; Chorny, M.; Koroukhov, N.; Danenberg, H. D.; Golomb, G. A new double emulsion solvent diffusion technique for encapsulating hydrophilic molecules in PLGA nanoparticles. J. Control. Release 2009, 133, 90–95.

31. Ravi Kumar, M. N. V.; Bakowsky, U.; Lehr, C. M. Preparation and characterization of cationic PLGA nanospheres as DNA carriers. BioMater. 2004, 25, 1771–1777.

32. Naghibzadeh, M.; Amani, A.; Amini, M.; Esmaeilzadeh, E.; Mottaghi-Dastjerdi, N.; Faramarzi, M. A. An Insight into the Interactions between a-Tocopherol and Chitosan in Ultrasound-Prepared Nanoparticles. J. NanoMater. 2010, ID 818717.

33. Schork, F. J.; Luo, Y. W.; Smulders, W.; Russum, J. P.; Butte, A.; Fontenot, K. Miniemulsion polymerization. Adv. Polym. Sci. 2005, 175, 129–255.

34. Galindo-Rodriguez, S.; Allemann, E.; Fessi, H.; Doelker, E. Physicochemical parameters associated with nanoparticle formation in the salting-out, emulsification-diffusion and nanoprecipitation methods. Pharm. Res. 2004, 21, 1428–1439.

35. Song, X.; Zhao, Y.; Hou, S.; Xu, F.; Zhao, R.; He, J.; Cai, Z.; Li, Y.; Chen, Q. Dual agents loaded PLGA nanoparticles: Systematic study of particle size and drug entrapment efficiency. Eur. J. Pharm. BioPharm. 2008, 69, 445–453.

36. Feczkó, T.; Tóth, J.; Dósa, G.; Gyenis, J. Influence of process conditions on the mean size of PLGA nanoparticles. Chem. Eng. Process. 2011, 50, 846–853.

37. Mainardes, R. M.; Evangelista, R. C. PLGA nanoparticles containing praziquantel: effect of formulation variables on size distribution. Int. J. Pharm. 2005, 290, 137-144.

38. Ven, H. V. d.; Vermeersch, M.; Matheeussen, A.; Vandervoort, J.; Weyenberg, W.; Apers, S.; Cos, P.; Maes, L.; Ludwig, A. PLGA nanoparticles loaded with the antileishmanial saponin β-aescin: Factor influence study and in vitro efficacy evaluation. Int. J. Pharm. 2011,

420, 122–132.

39. Arias, J. L.; Gallardo, V.; Gomez-Lopera, S. A.; Plaza, R. C.; Delgado, A. V. Synthesis and characterization of poly(ethyl-2-cyanoacrylate) nanoparticles with a magnetic core. J. Control. Release 2001, 77, 309-321.

40. Schwertmann, U.; Cornell, R. M. Iron oxides in the laboratory: preparation and characterization, 2nd ed.; Wiley-VCH: Weinheim, 2000.

41. Gómez-Lopera, S. A.; Plaza, R. C.; Delgado, A. V. Synthesis and Characterization of Spherical Magnetite/Biodegradable Polymer Composite Particles. J. Colloid. Interface Sci. 2001, 240, 40-47.